Mathematical modeling of operational modes of high-speed DACs

K.K. Khramov[1], V.V. Romashov[1]

[1]Vladimir State University, Orlovskaya street 23, Murom, Russia, 602264

Abstract. Mathematical modeling of the main operational modes used in high-speed digital-to-analog converters for digital generation of broadband signals is performed. The suggested variant of realization of impulse responses is investigated. The analysis of output signals of the digital signal generator in frequency domain is performed. The comparative characteristics of the considered modes are presented. Practical recommendations are given on the use of the considered operational modes for the formation of broadband signals.

Keywords: mathematical modeling, high-speed DAC, digital signal generation, broadband signal.

1. Introduction

The achievements of recent years in the field of microelectronics enabled the leading manufacturers of integrated circuits to significantly increase the conversion frequency of digital-to-analog converters (DACs) up to 12 GHz and create high-speed DACs that generate an analog signal directly at radio frequency (RF DAC). Currently, a wide range of such converters is available for developers of telecommunication devices and systems, for example: the MAX58xx and MAX196xx series from Maxim Integrated [1], AD91xx and AD97xx series from Analog Devices, Inc. [2], the DAC38RFxx series from Texas Instruments, Inc. [3].

The use of modern high-speed 12- to 16-bit DACs has made it possible to develop broadband multicarrier digital transmitters with a direct modulation at the radio frequency [4]. Such devices are used for the signal formation in cable television systems, broadband signals in microwave radars, and radio signals with digital modulation in telecommunication systems [5-8].

Practical interest is the modeling and analysis of operational modes that can be implemented in high-speed DACs.

2. Operational modes of high-speed DACs

As is known [9], the spectrum $\dot{S}_d(\omega)$ of DAC output signal is an infinite series of images of the spectrum $\dot{S}(\omega)$ of the fundamental frequency (signal)

$$\dot{S}_d(\omega) = \frac{\dot{S}_0(\omega)}{T} \sum_{n=-\infty}^{\infty} \dot{S}\left(\omega - \frac{2\pi n}{T}\right), \quad (1)$$

where $\dot{S}_0(\omega)$ – complex frequency response, determined by the transfer function of DAC; $T = 2\pi/\omega_T = 1/f_T$ – update clock rate.

The DAC's frequency response depends on impulse response (figure 1), so it will determine the amplitude distribution of the images in the spectrum of the output signal of the DAC [10, 11].

Traditionally, in a DAC, the signal is sampled by rectangular impulses of sample period T (figure 1(a)). This operational mode of the DAC is called non-return-to-zero (NRZ) mode. The frequency response in this case, taking into account the symmetry of the impulse response, is given by

$$\dot{S}_0(\omega) = \dot{S}_{\mathrm{NRZ}}(\omega) = A_0 T \frac{\sin(0.5\omega T)}{(0.5\omega T)} = A_0 T \sin c(0.5\omega T), \quad (2)$$

where A_0 – amplitude factor.

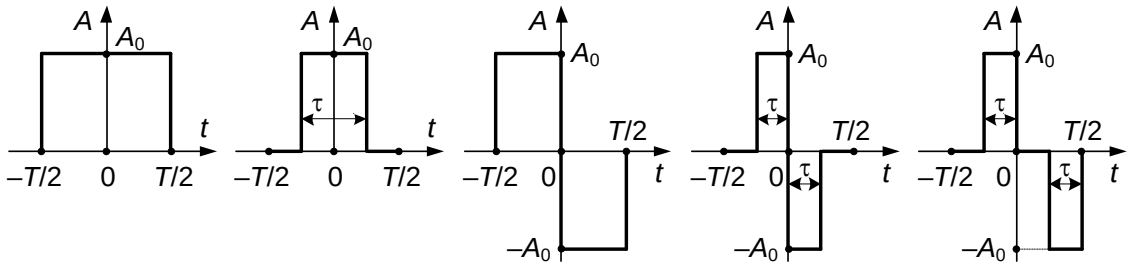

(a) (b) (c) (d) (e)

Figure 1. The high-speed DAC's impulse response for NRZ mode (a); RZ mode (b); RF mode (c); RFZ mode (d); and RFZ2 mode (e).

The frequency response $\left|\dot{S}_{\mathrm{NRZ}}(\omega)\right|$ normalized to A_0T is shown in figure 2 in decibels. It is obvious that the DAC's frequency response $\dot{S}_{\mathrm{NRZ}}(\omega)$ is proportional to the sin(*x*)/*x* function that has its zeros at multiples of the update clock rate ω_T. The same figure shows the signal spectrum $\left|\dot{S}_d(\omega)\right|$ at the output of the DAC in the synthesis of a harmonic signal with a fundamental frequency $\omega_0 = 0.2\omega_T$.

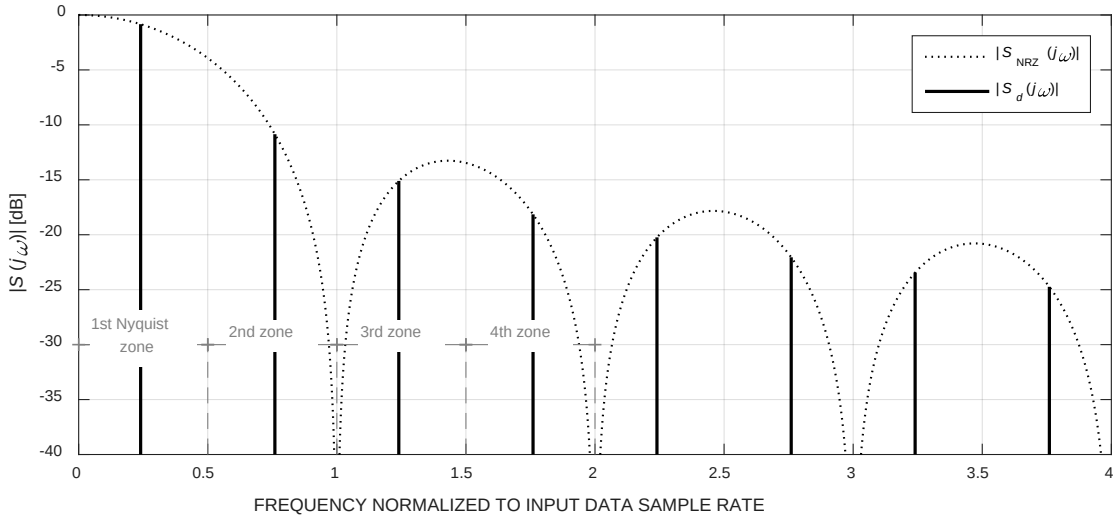

Figure 2. The normalized frequency response and output spectrum of DAC in the tone synthesis (NRZ mode).

The presence of images of the fundamental frequency in the spectrum of the DAC output signal makes it possible, by filtering, to synthesize signals at frequencies exceeding the clock frequency [11-13]. Using these images can reduce the input data sample rate and reduce the loss of DAC dissipation. The limitation is that the amplitude of the images located in second, third and fourth Nyquist zones is

at 10 to 20 dB less than the amplitude of the fundamental frequency (figure 2). In addition, if it is necessary to synthesize a broadband or multi-channel signal in these zones in the NRZ mode, a significant (up to 5 dB) unevenness in the band occurs.

High-speed DACs overcome these limitations. There are two main ways to solve these problems. The first is a significant increase the update clock rate of the DAC (Nyquist zones expansion) without changing the NRZ mode and the additional use of the correction function $x/\sin(x)$ to reduce the unevenness of DAC frequency response in the first Nyquist zone [2].

With the second way of increasing the clock rate of the DAC is accompanied by a change in the operational mode of the converter due to change in impulse response. The simplest way is to decrease each clock cycle τ (figure 1(b)). The operating mode of the DAC corresponding to this way is called return-to-zero (RZ) mode. As shown in [9-11], in this mode the spectrum $\dot{S}_{d2}(\omega)$ of the DAC output signal corresponds to the spectrum of the discrete signal in NRZ mode

$$\dot{S}_{d2}(\omega)=\dot{S}_{\mathrm{RZ}}(\omega)\sum_{n=-\infty}^{\infty}\dot{S}\left(\omega-\frac{2\pi n}{T}\right),$$

and the frequency response $\dot{S}_{\mathrm{RZ}}(\omega)$ in the RZ mode can be expressed through $\dot{S}_{\mathrm{NRZ}}(\omega)$ [10]:

$$\dot{S}_{\mathrm{RZ}}(\omega)=\frac{T}{2\pi}\int_{-\infty}^{\infty}\dot{S}_{q0}(\tilde{\omega})\dot{S}_{\mathrm{NRZ}}(\omega-\tilde{\omega})d\tilde{\omega}=\frac{A_0}{q}\cdot\frac{\sin\left(0.5\omega Tq^{-1}\right)}{\left(0.5\omega Tq^{-1}\right)}=\frac{A_0}{q}\cdot\sin\mathrm{c}\left(\frac{\omega T}{2q}\right) \quad (3)$$

where $\dot{S}_{q0}(\omega)=\frac{1}{q}\cdot\frac{\sin\left(0.5\omega Tq^{-1}\right)}{\left(0.5\omega Tq^{-1}\right)}$; $q=\frac{T}{\tau}$ – duty cycle of sample period.

It follows from expression (3) that an increase in duty cycle leads to an increase in the frequency response of the DAC by a factor of q due to the redistribution of the amplitudes of the images of the fundamental frequency. In practice, when implementing the RZ mode in high-speed DAC, the hardware value is $q=2$ [1-5].

The third operational mode used in some high-speed DACs is radio frequency (RF) or mix mode [1-2]. In its implementation, the DAC output signal is inverted during each clock cycle halfway through the clock period, i.e., $\tau=T/2$ (figure 1(c)). Using the conclusions obtained above and figure 1(c), we can write the expression for the complex frequency response at the DAC output in the RF mode

$$\dot{S}_{\mathrm{RF}}(\omega)=A_0\int_{-T/2}^{0}\exp(-\mathrm{i}\omega t)dt-A_0\int_{0}^{T/2}\exp(-\mathrm{i}\omega t)dt=\mathrm{i}A_0T\frac{\sin^2(0.25\omega T)}{(0.25\omega T)}. \quad (4)$$

Comparing the equations (2) and (4), we can conclude that in the RF mode the DAC update clock rate is twice the NRZ mode update clock rate. The multiplier $\sin(0.25\omega T)$ forms zero values of the frequency response at frequencies $\omega_k=2k\omega_T$, where k = 0, 1, 2, ... As follows from (4), the frequency response at the output of DAC in the RF mode is independent of the duty cycle q.

By reducing the duration of the bipolar pulses of the RF mode with respect to the time instant $t=0$, as shown in figure 1(d), the developers implement another operational mode of high-speed DAC, known as RFZ (radio frequency return-to-zero mode) [6]. The equation for the complex frequency response in this mode is obtained using (3) and (4):

$$\dot{S}_{\mathrm{RFZ}}(\omega)=A_0\int_{-\tau}^{0}\exp(-\mathrm{i}\omega t)dt-A_0\int_{0}^{\tau}\exp(-\mathrm{i}\omega t)dt=\mathrm{i}2A_0\frac{T}{q}\cdot\frac{\sin^2\left(0.5\omega Tq^{-1}\right)}{\left(0.5\omega Tq^{-1}\right)}. \quad (5)$$

For the last equation, the conclusions made for formulas (3) and (4) are valid. It is also obvious that for $q=2$ equation (5) coincides with (4), i.e. the RF mode is a special case of the RFZ mode with $\tau=T/2$.

In practical implementation of the RFZ mode in high-speed DAC, the value $q=4$ takes place [1], which requires a fourfold increase in the update clock rate in comparison with the NRZ mode.

Another operational mode of the high-speed DAC, conventionally called RFZ2, can be proposed and analyzed. In this mode, the duration of bipolar impulses, as well as in the RFZ mode, is $\tau < T/2$, however, the change in their duration is carried out with respect to the instants of time $t = 0$ and $t = T/2$ (figure 1(e)). The frequency response of the DAC output signal in this case will be determined by equation

$$\dot{S}_{\mathrm{RFZ2}}(\omega) = A_0 \int_{-\tau}^{0} \exp(-\mathrm{i}\omega t)dt - A_0 \int_{T/2-\tau}^{T/2} \exp(-\mathrm{i}\omega t)dt = \\ = \mathrm{i}2A_0 \frac{T}{q} \cdot \frac{\sin\left(0.5\omega T q^{-1}\right)}{\left(0.5\omega T q^{-1}\right)} \sin\left(\frac{\omega T}{4}\right) \exp\left[\mathrm{i}\omega T\left(\frac{1}{2q}+\frac{1}{4}\right)\right]. \quad (6)$$

Structures of expressions (5) and (6) are similar, but in contrast to formula (5), in the last expression, instead of the multiplier $\sin\left(0.5\omega T q^{-1}\right)$, there appears the multiplier $\sin(0.25\omega T)$, which gives fixed zeros of the function $\dot{S}_{\mathrm{RFZ}}(\omega)$ at frequencies $\omega_k = 2k\omega_T$, where k = 0, 1, 2, ... , and the multiplier exp[...], which is determined by the offset of impulse response along the time axis.

3. Comparative analysis of the considered operational modes

Let us analyze the frequency responses plotted from expressions (2)-(6). In figure 3 and figure 4 are combined graphics of the frequency responses of the DAC output signals for different operational modes for two values of the duty cycle $q = 2$ and $q = 4$. The resulting graphs are normalized to the level $\left|\dot{S}_{\mathrm{NRZ}}(0)\right|$ of NRZ mode and are expressed in decibels.

As follows from the above graphs, in all modes (RZ, RF, RFZ, RFZ2), the amplitude values of some spectral components of 2...8 Nyquist zones can be increased by several decibels due to the energy redistribution in the spectrum of the DAC output signal, mainly from the first zone. In RZ mode, the DC level depends on the duty cycle: $S_{\mathrm{RZ}}(0) = 20\lg(q)$. In the RF, RFZ and RFZ2 modes, there is no DC component in the output signal. For $q = 2$ (figure 3), the frequency responses $S_{\mathrm{RF}}(\omega)$, $S_{\mathrm{RFZ}}(\omega)$ and $S_{\mathrm{RFZ2}}(\omega)$ of the DAC output signal are coincide and sufficiently flat in the second and sixth Nyquist zones. It allows to synthesize in these zones an output signal with bandwidth of up to $0.5\omega_T$.

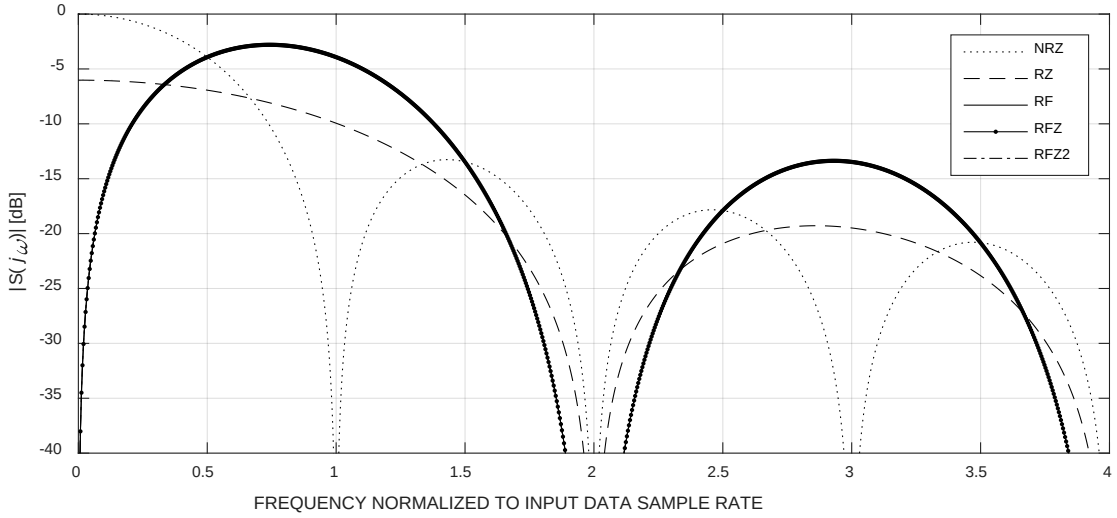

Figure 3. The high-speed DAC's normalized frequency responses for different operational modes at $q = 2$.

With an increase in the duty cycle to $q=4$ (figure 4), the first lobe of the frequency response $S_{\mathrm{RFZ}}(\omega)$ is expands, and it becomes possible to form a broadband signal covering 2...5 Nyquist zones. However, the level of this signal will not exceed a value of minus 9 dB relative to the full scale of the DAC. In the RFZ2 mode, it is possible to synthesize a broadband signal covering the second and third Nyquist zones, as well as in the sixth zone.

A similar drawback of the RF and RFZ2 modes is the impossibility of synthesizing a signal in the vicinity of the frequency $\omega=2\omega_T$.

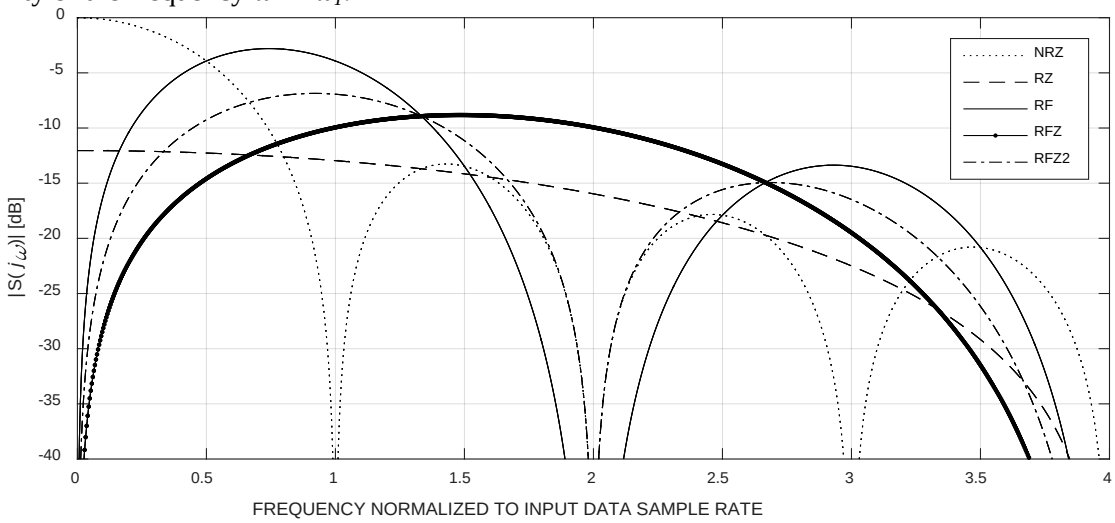

Figure 4. The high-speed DAC's normalized frequency responses for different operational modes at $q=4$.

In [10], a function $R(\omega,q)$ was introduced, which is equal to the ratio of the modulus of a given frequency response to the function $\left|\dot{S}_{\mathrm{NRZ}}(\omega)\right|$. The function $R(\omega,q)$ allows you to perform a quantitative analysis of the relative changes in the amplitudes of spectral components with a change in the duty cycle and the fundamental frequency of the DAC output signal. We write the expression $R(\omega,q)$ for the considered modes:

$$R_{\mathrm{RZ}}(\omega,q)=20\lg\left(\frac{\left|\dot{S}_{\mathrm{RZ}}(\omega)\right|}{\left|\dot{S}_{\mathrm{NRZ}}(\omega)\right|}\right)=20\lg\left(\left|\frac{\sin\left(0.5\omega Tq^{-1}\right)}{\sin\left(0.5\omega T\right)}\right|\right); \tag{7}$$

$$R_{\mathrm{RF}}(\omega,q)=R_{\mathrm{RF}}(\omega)=20\lg\left(\frac{\left|\dot{S}_{\mathrm{RF}}(\omega)\right|}{\left|\dot{S}_{\mathrm{NRZ}}(\omega)\right|}\right)=20\lg\left(2\frac{\sin^2\left(0.25\omega T\right)}{\left|\sin\left(0.5\omega T\right)\right|}\right); \tag{8}$$

$$R_{\mathrm{RFZ}}(\omega,q)=20\lg\left(\frac{\left|\dot{S}_{\mathrm{RFZ}}(\omega)\right|}{\left|\dot{S}_{\mathrm{NRZ}}(\omega)\right|}\right)=20\lg\left(2\frac{\sin^2\left(0.5\omega Tq^{-1}\right)}{\left|\sin\left(0.5\omega T\right)\right|}\right); \tag{9}$$

$$R_{\mathrm{RFZ2}}(\omega,q)=20\lg\left(\frac{\left|\dot{S}_{\mathrm{RFZ2}}(\omega)\right|}{\left|\dot{S}_{\mathrm{NRZ}}(\omega)\right|}\right)=20\lg\left(2\left|\frac{\sin\left(0.5\omega Tq^{-1}\right)\cdot\sin\left(0.25\omega T\right)}{\sin\left(0.5\omega T\right)}\right|\right). \tag{10}$$

To analyze the influence of the duty cycle q on the change in the levels of the images when synthesizing a tone signal with the fundamental frequency $\omega_0=0.24\omega_T$, we plot the functions (7)-(10) for $\omega=\mathrm{const}$ (figure 5).

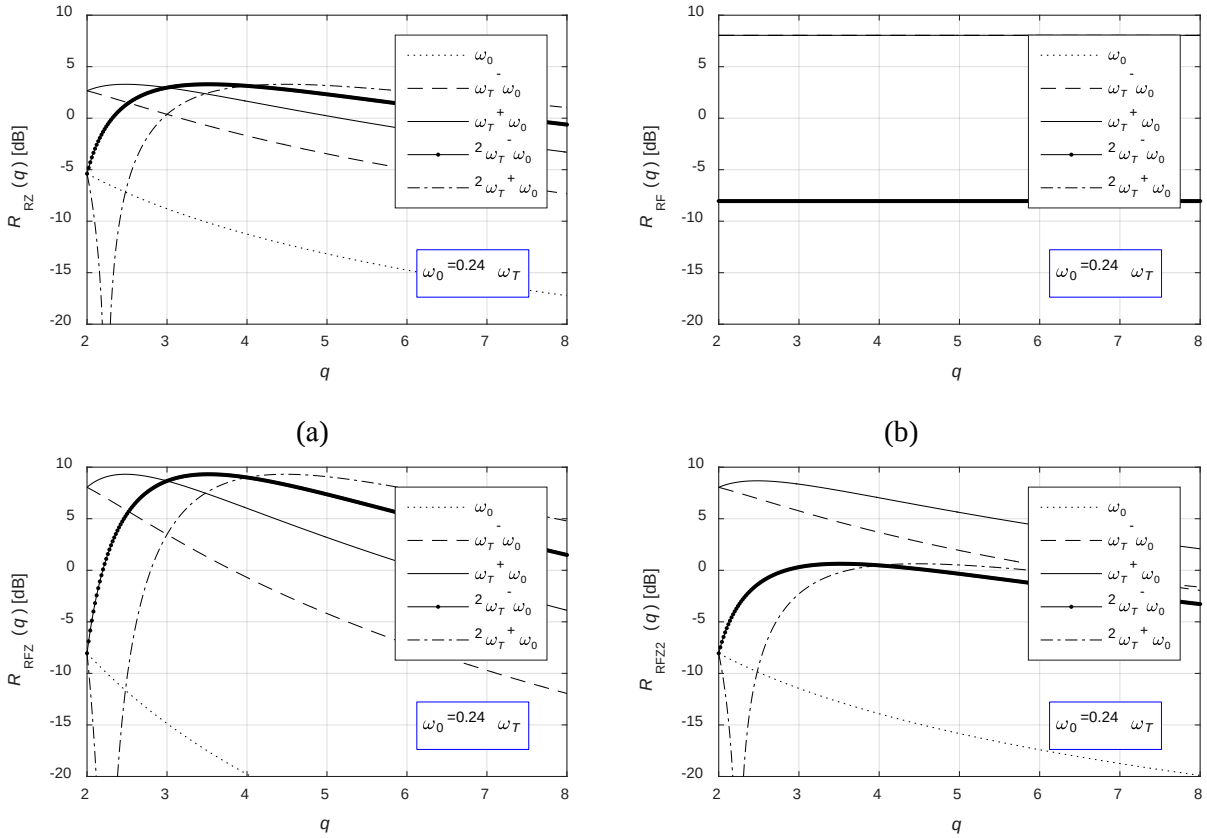

Figure 5. The functions of the relative changes in the amplitude of the images at the output of the DAC with the fundamental frequency $\omega_0 = 0.24\omega_T$ and a change in the duty cycle q for different operational modes: RZ (a), RF (b), RFZ (c), and RFZ2 (d).

The curves in figure 5 allow to determine for each operational mode the maximum relative amplitude value of any image of the DAC output signal with an appropriate choice of duty cycle q. For example, for the RZ mode with the ratio $\omega_0 = 0.24\omega_T$, it is theoretically possible to increase the amplitude of any image by 3.3 dB with respect to the NRZ mode, and for the RFZ mode such increase is 9.3 dB. In RF mode, the relative level of images does not depend on q and has constant relative values: minus 8.05 dB – for images near the frequencies $k\omega_T$, where k = 0, 2, 4, ..., and 8.05 dB – for images in the vicinity of the frequencies $(k+1)\omega_T$. In the RFZ2 mode, the $R(q)$ values have two limiting values: 8.7 dB for images in the second and third Nyquist zones and 0.63 dB for the images in the fourth and fifth zones.

In general, the relative levels of the images $R(\omega, q)$ will increase for all the considered DAC modes with decreasing fundamental frequency ω_0. This is illustrated by the graphs in figure 6, where the functions $R(\omega)\big|_{q=const}$ are given for a fixed duty cycle q.

As follows from the graphs in figure 6(a), for q = 2, the functions $R(\omega)\big|_{q=const}$ for the RF, RFZ and RFZ2 modes are the same, which also follows from equations (8)-(10). In the RZ, RFZ and RFZ2 modes in the vicinity of frequencies $kq\omega_T$, where $k = 0, 1, 2, \ldots$, there is a relative decrease in the level of the frequency responses of the DAC output signal. In the RF mode, such decrease does not depend on q and has place in the vicinity of the frequencies $k\omega_T$.

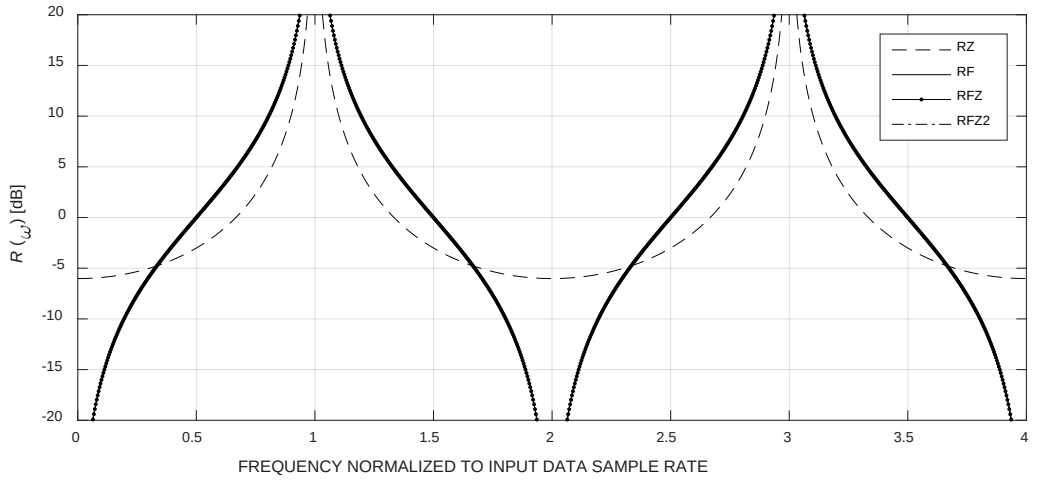

(a)

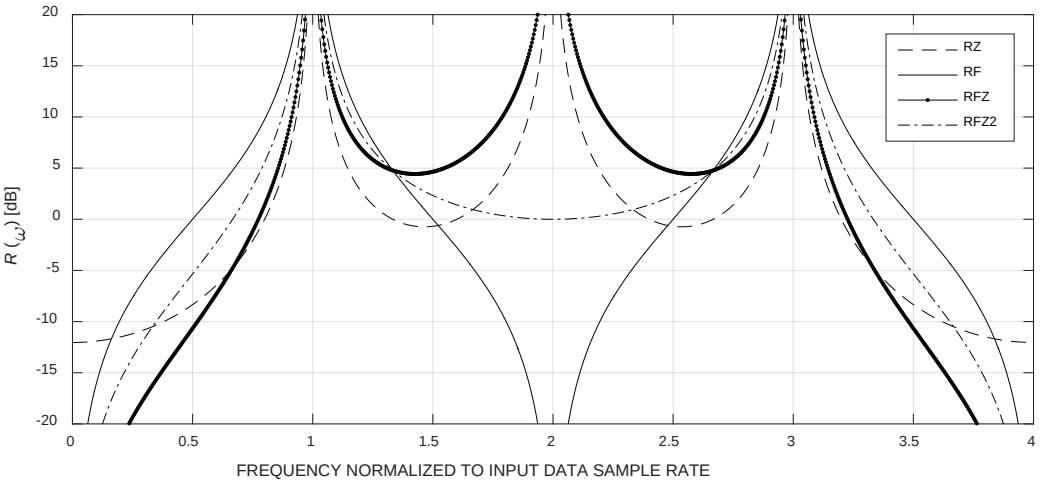

(b)

Figure 6. The functions of relative changes in the frequency responses of the DAC output signal for various operational modes for $q = 2$ (a) and $q = 4$ (b).

4. Simulation of high-speed DAC

The discrete model of a high-speed DAC based on the impulse responses and equations obtained above was created in Simulink (figure 7). This model synthesizes signals for various operational modes of high-speed DAC. The broadband FM signal was selected as the input signal. The model allows you to set the update clock rate, duty cycle, the type of the input signal, the main frequency and bandwidth of the input signal, and also select the operational mode of the DAC.

Figure 8 shows the time diagrams of the shaper operation and the spectrums of DAC when simulating the RFZ mode. The obtained operation results correspond to impulse responses (figure 1) and frequency responses (figure 4) for this mode.

The DAC model can be used to study various operational modes of high-speed DAC, to select optimal parameters for digital-to-analog conversion in the synthesis of broadband signals, to define the parameters of filter at the output of the DAC.

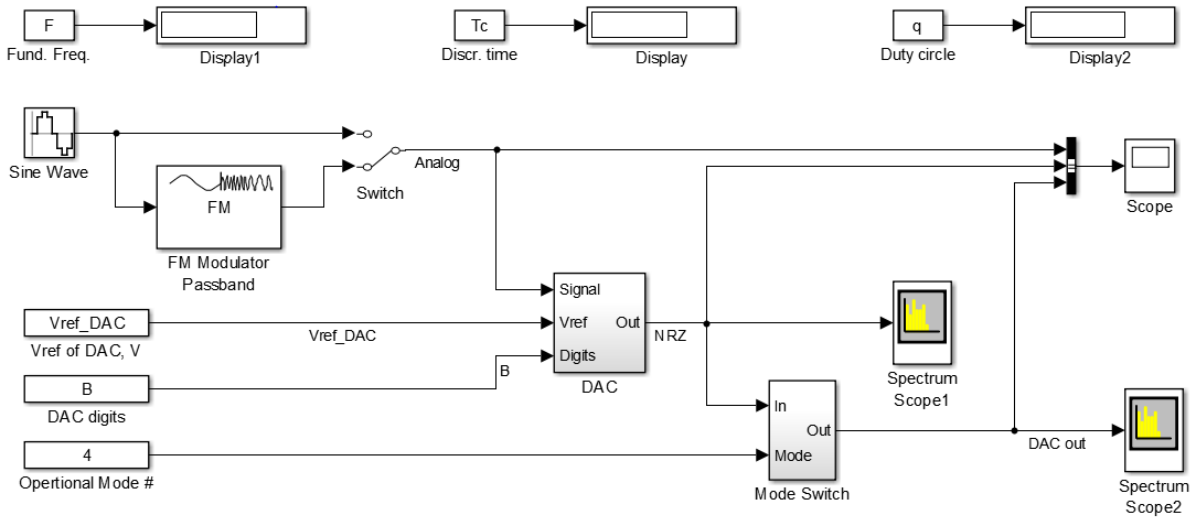

Figure 7. The model of a high-speed DAC.

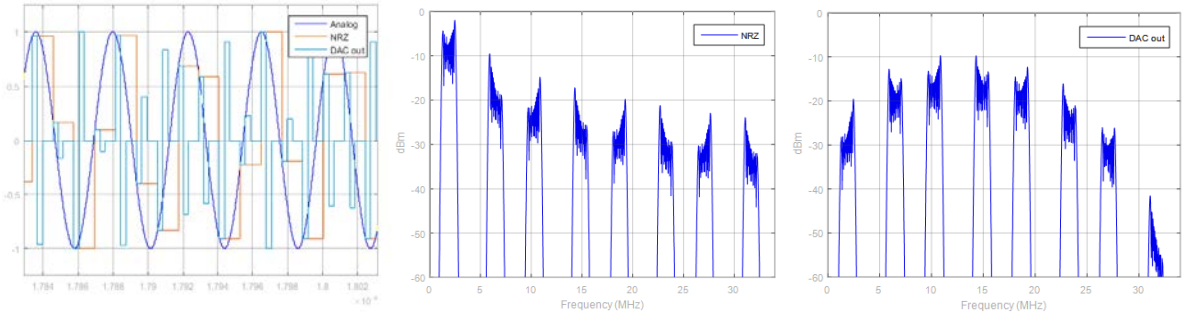

Figure 8. The results of simulation of high-speed DAC in RFZ mode at $q = 4$.

5. Conclusion

Thus, the considered variants of impulse responses allow selecting the most appropriate operational mode of high-speed DAC for synthesizing broadband (multi-frequency) radio signals with the required parameters. The obtained mathematical expressions make it possible to calculate the relative level of the DAC output signal and frequency response unevenness in the band for any values of the DAC fundamental frequency and the pulse duty cycle.

The implementation of the considered operational modes using FPGA or DSP opens the possibility of direct digital synthesis of broadband radio signals in the VHF and UHF bands.

6. References

[1] Maxim Integrated, Web Site [Electronic resource]. – Access mode: https://para.maximintegrated.com (10.11.2017).

[2] Analog Devices, Inc., Web Site [Electronic resource]. – Access mode: http://www.analog.com/en/index.html (10.11.2017).

[3] Texas Instruments, Inc., Web Site [Electronic resource]. – Access mode: http://www.ti.com (10.11.2017).

[4] Kuckreja, A. High-Speed DACs ease transmitter designs / A. Kuckreja, O. Geir. – Microwave & RF, August, 2010.

[5] Overhoff S. Direct-Sampling DACs in Theory and Application / Stephanie Overhoff // Application note 5446. – Access mode: https://www.maximintegrated.com/en/app-notes/index.mvp/id/5446.

[6] Synchronizing Multiple High-Speed Multiplexed DACs for Transmit Applications. Application note 3901. – Access mode: https://www.maximintegrated.com/en/app-notes/index.mvp /id/3901.

[7] Romashov, V.V. The Reference Shapers of the Transmitter Exciter Using Images of Fundamental Frequency / V.V. Romashov, K.K. Khramov // Methods and Devices of Information Transmission and Processing. – 2011. – Vol.13. – P. 44-47. (in Russian).
[8] Romashov, V.V. The Frequency Planning of Radio Signal Shapers Based on Direct Digital Synthesizers / V.V. Romashov, K.K. Khramov, A.N. Doktorov // Radio and Telecommunication Systems. – 2012. – Vol. 4. – P. 10-15. (in Russian).
[9] Sergienko, A.B. Digital Signal Processing. – St. Petersburg: "Piter" Publisher, 2002. – 608 p.
[10] Romashov, V.V. Formation of Signals in VHF/UHF Ranges at Use of a Method of Direct Digital Synthesis of Frequencies / V.V. Romashov, K.K. Khramov // Radioengineering. – 2007. – Vol. 6. – P. 39-41. (in Russian).
[11] Khramov, K.K. Effective use of spectrum images in VHF and UHF bands at direct digital synthesis of frequencies / K.K. Khramov // Methods and Devices of Information Transmission and Processing. – 2009. – Vol. 11. – P. 108-112. (in Russian).
[12] Romashov, V.V. The Use of Images of DDS in the Hybrid Frequency Synthesizers / V.V. Romashov, L.V. Romashova, K.K. Khramov, K.A. Yakimenko // 24th International Crimean Conference Microwave and Telecommunication Technology Conference Proceedings. – 2014. – P. 302-303.
[13] Romashov, V.V. The Use of Images of DDS Fundamental Frequency for High-Frequency Signals Formation / V.V. Romashov, K.K. Khramov, A.N. Doktorov, // 24th International Crimean Conference Microwave and Telecommunication Technology Conference Proceedings. – 2014. – P. 310-311.